Laboratory tests of floor-to-frame connections for controlled rocking steel braced frames

Taylor C. Steele[1] and Lydell D. A. Wiebe[2]

[1] Ph.D. Candidate, Department of Civil Engineering, McMaster University - Hamilton, ON, Canada.
[2] Associate Professor, Department of Civil Engineering, McMaster University - Hamilton, ON, Canada.

ABSTRACT

Controlled rocking steel braced frames (CRSBFs) have been proposed as a low-damage seismic force resisting system with reliable self-centring capabilities. While the design of the rocking joint and the frame members in CRSBFs has been researched extensively, relatively little research has been completed on how to connect the CRSBF to the gravity framing to transfer the inertial forces. The connections between the floor diaphragms and the controlled rocking system must be capable of transferring large lateral forces during seismic excitation. At the same time, to prevent damage to the floor slabs, they must also able to accommodate the relative vertical displacement between the two systems due to the uplift of the rocking system. One past experimental study on CRSBFs implemented a frictional bearing interface between the gravity columns and the frame, but this detail has yet to be implemented in real buildings with CRSBFs. The floor-to-frame connections in other experimental studies were adequate for laboratory purposes, but they were not tested or intended for full-scale applications in practice. This paper presents the experimental results for three different floor-to-frame connections tested in a one-storey CRSBF prototype at 60% scale. A 1000 kN actuator was used to apply the lateral load to the structures, while two 500 kN and one 1000 kN vertical actuators were used to simulate the downward force from the frame above the first storey. The connections are evaluated using cyclic static tests. The first connection is a bearing plate connection (BPC) that transfers the lateral forces through bearing in one direction only between a curved male plate on a flat female plate. The second connection is a sliding pin connection (SPC) that transfers the lateral loads from the gravity framing to the CRSBF through bearing of a single pin on steel plates in two directions, while also permitting uplift through sliding of the pin along the bearing surface within long slotted holes. The behaviour and performance of each connection are discussed, and the influence of each connection on the global behaviour of the CRSBF subassembly is quantified. A simple calibrated model is proposed to provide a comparison between the idealised flag-shaped hysteresis and the experimental results. The experimental results and idealised model are generally in good agreement when the shape of the hysteresis more closely emulates the idealised flag shape.

Keywords: controlled rocking steel braced frames, floor-to-frame connections, large-scale experimental tests, cyclic static tests

INTRODUCTION

Controlled rocking steel braced frames (CRSBFs) have emerged with increasing interest as high-performance seismic force resisting systems that mitigate structural damage during earthquakes. Structural damage is mitigated by concentrating the nonlinear displacement demands on the structure at the base through a controlled rocking mechanism, where a combination of energy dissipation devices and post-tensioning allow the frame to uplift once the overturning resistance is exceeded, dissipate energy, and provide a restoring force to the frame while rocking. The resulting hysteretic behaviour of CRSBFs is characterized by a flag-shaped hysteresis, where the residual displacements are essentially zero after the earthquake.

Figure 1 shows the two main proposals for the design and implementation of CRSBFs with complete building systems (e.g. in [1]). One option is to design a CRSBF that is coupled with the gravity framing, thereby imposing uplifting displacements on the floor system tributary to the columns of the braced bay [2, 3, 4]. The gravity loads carried by the floor system are transferred into the CRSBF and contribute to the overturning resistance of the braced bay, reducing the amount of post-tensioning or energy dissipation required to resist wind loads and inertial forces under small earthquakes. CRSBFs that are coupled with the gravity framing in this way can lend themselves to the seismic retrofit of deficient low-rise concentrically braced frame buildings [5]. The rotation and axial force demand on the collector beams framing into the CRSBF can generally be accommodated using connection details that are consistent with current steel design codes and standards such as sliding holes or a single pin [6]. Gledhill et al. [2] and Tait et al. [3] present case studies during which CRSBFs were designed and constructed to be integrated with the gravity framing. However, for such CRSBFs, concerns have been expressed in the literature regarding the dynamic effects from impact of the uplifting columns on the foundation, and regarding localized damage of the floor slabs from the rotational demands placed on the floor system during uplift [1].
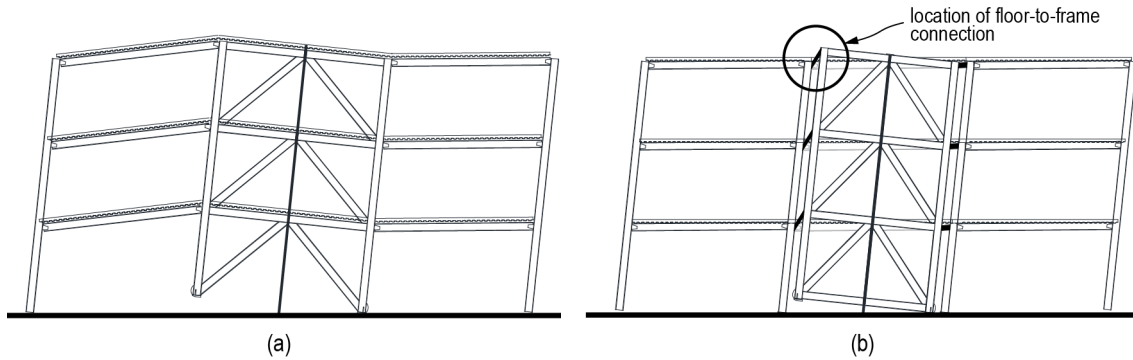
Figure 1. Controlled rocking steel braced frame (a) coupled with gravity framing and (b) decoupled from gravity framing.

Figure 1(b) shows a second option to address the concerns associated with the integrated option, where the CRSBF is placed between gravity columns of the braced bay with special connection details that allow the frame to rock without imposing uplift on the adjacent gravity framing, thereby decoupling them from one another [7, 8, 9, 10, 11]. With this layout, the CRSBF does not carry any tributary gravity loads and it has the potential to mitigate the localized slab damage to the floor system and the dynamic effects of column impact. However, the additional detailing required for connections between the gravity framing and the CRSBF are not yet addressed by steel design codes and standards. For CRSBFs that are decoupled from the gravity framing, Roke et al. [10] suggested providing a bearing stub protruding from the gravity framing that would transfer the inertial forces from the floor diaphragm to a wear plate on the CRSBF; this connection allowed the force to be transferred to the CRSBF through bearing of the stub on the wear plate while accommodating the relative uplift through sliding. This connection worked well in the experimental program and acted as means of dissipating energy through friction during rocking with minimal damage to the bearing or the wear plate [10]. However, the out-of-plane restraint was not self-contained in the connection detailing, and the design, performance and influence of the connections on the CRSBF behaviour was not the focus of the research program. Eatherton and Hajjar [8] suggested using either shear-plate connections between the collector beams and the beams of the CRSBF or a yoke-and-roller at either end of the CRSBF to transfer the inertial forces in bearing and accommodate the uplift of the frame. The shear-plate connections would transfer the inertial forces into the frame through shear while accommodating the uplift through flexural hinging. For the yoke-and-roller detail, the uplift could be accommodated through the rolling action without generating significant friction at the interface. Removing the friction at the interface would mean that the overturning response of the CRSBF would not depend on the connection detail, resulting in one less component to consider for the design of the base rocking joint, and that no additional energy would be dissipated by the connection while rocking. In summary, among the floor-to-frame connections that have been proposed for CRSBFs that are decoupled from the gravity framing, only the bearing and friction plate option has been validated experimentally [10], and no design procedure was proposed for that detail.

This paper presents proposals and experimental results for two new connection details between the gravity framing and CRSBFs that are decoupled from the gravity framing to transfer the inertial forces and accommodate the relative vertical displacements. The proposed connections and the experimental program are introduced. An idealised calibrated model is proposed to provide a comparison between the idealised flag-shaped hysteresis and the experimental results. The behaviour and performance of each connection are discussed, and the influence of each connection on the global behaviour of the CRSBF subassembly is quantified. Rationale for two mechanisms for one of the connections is presented and the influence of these mechanisms on the global response of the CRSBF test setup is discussed.

PROPOSED CONNECTION DETAILS

Figure 2 shows the two details that were tested during the experimental program and are discussed in this paper. The first connection was a bearing plate connection (BPC), which had two main components as shown in Figure 2(a). The female part of the connection had two 25 mm side plates that were welded to a 25 mm main plate that was bolted to the CRSBF column, which will here forth be referred to as the CRSBF vertical strut to emphasize that it does not support tributary gravity loads. A 50 mm plate was placed between the side plates to provide a bearing surface away from the CRSBF vertical strut. The male part of the connection was a 50 mm thick curved plate to match the spacing between the side plates and only contacts the female side in bearing. The height of the bearing plate on the female components was specified such that the bearing point of the male plate would remain in contact with the bearing surface for drifts of up to 4%. This connection is like that proposed by Roke et al. [10] in that the forces are transferred through bearing in one direction only, and the relative uplifts are accommodated through sliding. However, the addition of the side plates provides out-of-plane restraint between the CRSBF and the gravity
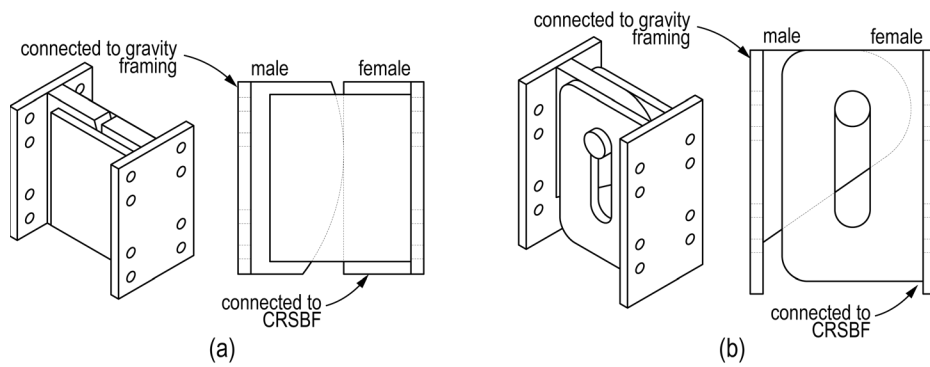
Figure 2. Proposed floor-to-frame connection details for testing (a) bearing plate connection (BPC) and (b) sliding pin connection (SPC).

framing, so no additional mechanisms are required for out-of-plane restraint. All the plates were connected using fillet welds along the contact surfaces.

The second connection (Figure 2(b)) was a sliding pin collection (SPC). The SPC is composed of three main components: the female side of the connection has two 25 mm thick side plates with 69 mm wide long slotted holes along their height, both welded to a perpendicular 25 mm thick main plate bolted to the face of the CRSBF vertical strut. The male part of the connection was a single tapered plate with one 69 mm circular hole that was welded to a perpendicular main plate bolted to the face of the gravity column. The last component was a single steel pin that was inserted through the male and female components. The male component, which is connected to the gravity column, transfers the load into the female component connected to the CRSBF through bearing, and accommodates the relative uplifts through sliding or rolling. The side plates are also intended to provide out-of-plane restraint between the gravity framing and the CRSBF, and cotter pins were placed through the ends of each pin with a washer to keep the pin from sliding out from the connection. The location of the pin in the connection at rest was 25 mm below the top of the sliding hole and 170 mm above the bottom of the sliding hole so that the pin had appropriate clearance to travel while the frame rocked in both directions. This connection is like the yoke-and-roller detail proposed by Eatherton et al. [8], in that the pin would be capable of rolling in the hole on the male end of the connection to accommodate the relative uplift, but the pin can transfer the force in both compression and tension whereas the yoke roller would only transfer the load through compression.

CONTROLLED ROCKING STEEL BRACED FRAME TEST SETUP

The Simulator for Innovative Next Generation Structural Systems (SINGSS) was recently commissioned at McMaster University's Applied Dynamics Laboratory for large-scale structural testing. Figures 3(a) and (b) show the rendering and photo of the SINGSS, respectively. The horizontal displacement was applied using a 1000 kN capacity 20-inch stroke actuator under displacement control. The vertical load and overturning moment were controlled through two 500 kN capacity 12-inch stroke actuators at the North end of the setup, and one 1330 kN actuator at the South end. Out-of-plane support was provided to the loading beam using two 3-inch diameter 10-inch stroke implement cylinders. The out-of-plane displacement was measured and held at the initial position using laser displacement transducers.

Figure 3 shows the CRSBF sub-assembly in the SINGSS setup. The CRSBF sub-assembly used to test the connections included a one-storey CRSBF with the adjacent gravity framing. The assembly was a 60% scale model based primarily on the NIST archetypes for braced frame buildings [12]. The scaled bay width was 5.5 m, and the width of the CRSBF was 4.56 m to fit between the gravity columns. The scaled height of the storey from the base to the centre line of the collector beams was 2.86 m. The CRSBF was a prefabricated welded frame comprising W250x73 sections as the frame members, all of which were designed to remain elastic under the maximum possible loading from the hydraulics.

The tributary gravity framing included one gravity column at each end of the frame and two collector beams that passed on either side of the CRSBF. The columns were also W250x73 sections, and the bases of the gravity columns were attached to the foundation by a 3-inch pin through the CRSBF bumper plate to accommodate rotation while generating negligible bending moment. The pin at the base is not a recommended detail for real construction, but this was done to prevent any unintended contribution to the lateral resistance during the tests. The collector beams between the gravity columns were W460x123 steel sections and were connected by plates with slotted holes using a detail proposed by Eatherton et al. [8] to resist the axial forces and accommodate the rotation of the beams relative to the gravity columns under large lateral displacements.

CRSBFs that are decoupled from the gravity framing generally rely on post-tensioning to provide a restoring force and self-centre the system after rocking, and supplemental energy dissipation to limit the peak displacements while rocking. For the
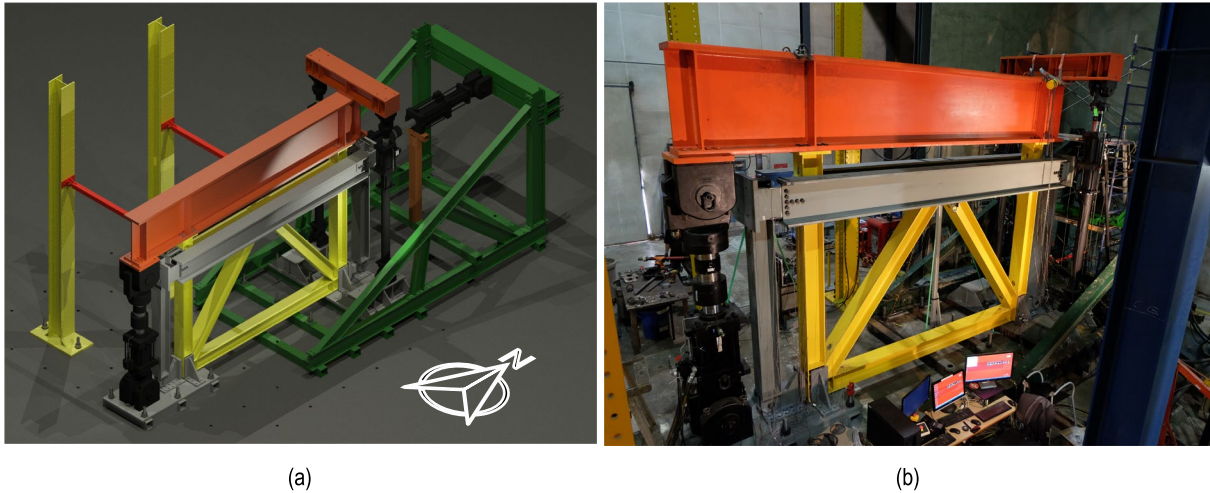
(a)   (b)

Figure 3. Layout of test setup: (a) AutoCAD rendering and (b) and as-built photo of setup.

tests presented in this study, the role of the post-tensioning is simulated by the vertical actuators. Supplemental energy dissipation devices were omitted in the experimental setup to isolate the influence of the connection detail on the hysteretic response of the CRSBF and to quantify how much energy dissipation would be provided by the connection details themselves while rocking.

Lateral displacements of the sub-assembly and the uplifts of the CRSBF vertical struts were measured using 250 mm string potentiometers. The connection forces were determined from equilibrium using the frame member forces that were calculated from the strain gauge readings at each member end, and the overturning moment was calculated by multiplying the CRSBF base shear by the height above the base to where the lateral force was transferred from the gravity framing to the CRSBF.

CALIBRATED IDEALIZED MODELS

The experimental results for each connection were used to calibrate an idealised model using the equivalent average energy dissipation ratio, β, which is defined as twice the overturning moment resistance from the energy dissipating elements to the total overturning resistance of the CRSBF, and the equivalent energy dissipation overstrength factor, f, defined in this paper as the ratio of the maximum base overturning moment to the base rocking moment observed from the experimental results. The equivalent average β value was calculated by dividing the total energy dissipated by the sum of the magnitude of the peak base rotation at each cycle to find the average base moment from the energy dissipation in the connections (i.e. the height of the flag in the flag-shaped hysteresis) and dividing that value by the idealised base rocking moment; the idealised base rocking moment was calculated by adding the computed average base moment from the energy dissipation in the connections to the idealised contributions of the frame self-weight and the post-tensioning, as simulated by the initial vertical force applied by the actuators. The maximum base moment was calculated at the peak base rotation for each test by including the energy dissipation overstrength factor, f, determined from the experimental results as the maximum overturning moment divided by the idealised rocking moment. These parameters were selected both because they can be used to define an idealised flag-shaped hysteresis, and because they are important parameters for both the design of the base rocking joint and of the capacity protected frame members [5, 9, 13, 14].

EXPERIMENTAL RESULTS

Bearing Plate Connection (BPC)

Figure 4(a) and (b) show the overturning moment-base rotation hysteresis loops for the CRSBF with the bearing plate connection installed between the gravity framing and the CRBSF for when 270 kN and 405 kN of vertical force was applied by the actuators, respectively. For comparison, the contribution of the vertical actuators to the overturning resistance (representing $M_W + M_{PT}$) and the hysteresis from the idealised model are also included in the figure. As expected, the overturning moment at uplift and the energy dissipated were larger when higher vertical loads were applied, but the equivalent β and f values were similar. The equivalent average β values were 0.366 and 0.357, respectively, and the equivalent f values were 1.22 and 1.18, respectively. The response of the connections was not perfectly smooth, but given that the bearing surfaces were torch-cut rather than machined, the response was reasonably consistent. Additional tests on the BPC not presented here showed that the response became smoother over time as the contact between the steel plates ground away the uneven surfaces. Part of the roughness in the response was caused by the widening of the curved plate at the bearing surface, which caught and
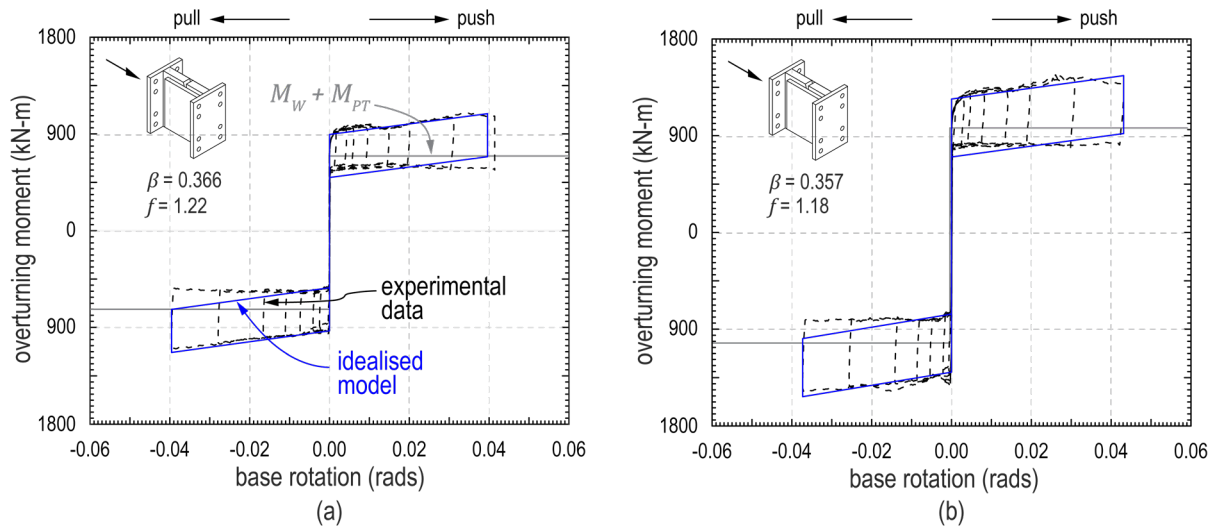
Figure 4. Cyclic static results for BPC under (a) 270 kN and (b) 405 kN of vertical load.

scraped on the side plates as one component slid relative to the other. This can be mitigated by using a wider dimension between the side plates to accommodate this deformation.

The BPC carried up to 600 kN of lateral force during the tests, which is 20% larger then Figure 4 would suggest because the results omit the contribution of the vertical actuator breakaway torque to the lateral resistance, which had to pass through the connection between the CRSBF and the gravity framing. The BPC also accommodated the relative uplifts at base rotations beyond 4%. The maximum uplifts were limited by the stroke of the vertical actuators in these tests, and not by the connections themselves. No slip was observed between the CRSBF and the female component of the BPC or between the gravity column and the male component of the BPC.

The calibrated idealised model worked well to represent the experimental results, as the shape of the hysteresis matched well. However, the idealised model is limited to a single secondary stiffness, and while this matched the secondary stiffness of the hysteresis obtained from the experimental results, it did not match the stiffness on the return from the peak base rotation to its initial position. Different stiffnesses in the flag portion of the hysteresis are typical of friction-based connections, where the amount of resistance is directly proportional to the applied lateral force [9].

Sliding Pin Connection (SPC): Initial Mechanism

Figure 5 shows the hysteretic response for when the sliding pin connection (SPC) was used between the gravity framing and the CRSBF. The hysteresis was not symmetric as intended; the force required to push the frame to a given base rotation was as much as twice the force required to pull the frame to the same base rotation in the opposite direction. This was because the two connections at either side of the CRSBF did not share the load equally; instead, the connection on the north end of the CRSBF and immediately adjacent to the horizontal actuator that was loading the specimen transferred essentially all of the force into the CRSBF. The tolerance in the bolt holes at the collector beam-column connections and in the pin holes and sliding holes provided relief to the connection at the south end of the frame, preventing it from engaging in bearing on the side plates bolted to the CRSBF.

In addition, the first cycle of the test shown in Figure 5(a) beyond the previous peak during the push cycles was always different from the following cycles, reaching higher forces with a steeper slope. This was because the sliding holes in the side plates were torch cut by the steel fabricator, which left a non-perpendicular surface that was rougher than a machined or milled surface would have been. Because the bearing surface was not perpendicular to the pin, the steel yielded in bearing under the initial stress concentration between the pin and the edge of the slotted hole, and the sliding motion of the pin scraped the steel away from the surface. The response was more repeatable during the following cycles because the bearing surface was smoother and squared-off after the initial cycle, but the overall response was rougher than what would be desirable for the design of CRSBFs.

The slotted hole in the side plates also prevented the frame from rotating beyond just less than 0.04 rad; this point is observable on both hysteresis loops as an abrupt stiffness change. This could serve as an intentional lockup mechanism to prevent excessive displacements in CRSBFs during large earthquakes, but the additional forces imposed on the frame members may be detrimental if not accounted for in the design.
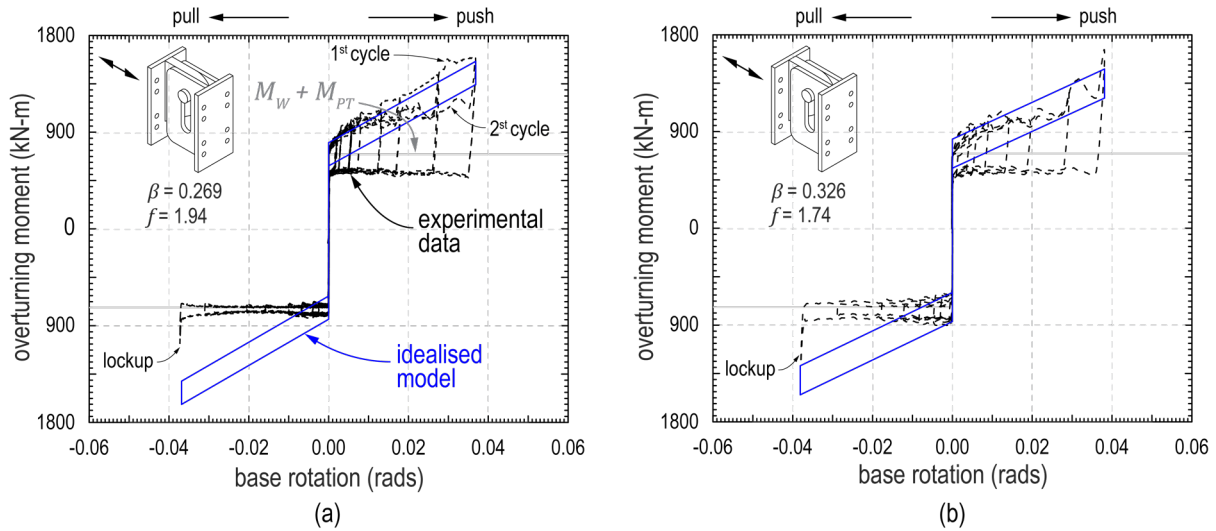
Figure 5. Cyclic static results for SPC for intended load transfer at uplifting end: (a) first test and (b) second test, both under 270 kN of vertical load.

The idealised model did not reflect the experimental results well because of the asymmetry and the roughness of the hysteresis from the experimental results. Despite this anomaly, the global building response could be still symmetric if two CRSBFs were used with the connections on opposite ends of the CRSBFs. A second assembly would still be required at the opposite ends for out-of-plane restraint, although the pin may be excluded as this connection would not be needed to transfer any from the gravity framing into the CRSBF. Overall, the observed behaviour for this connection was not as predictable as intended.

Sliding Pin Connection (SPC): Revised Mechanism

To use connections that dissipate energy and add to the post-uplift stiffness as demonstrated in the tests presented above, designers must to be able to predict the behaviour of the connection before proportioning the supplemental energy dissipation and post-tensioning elements. One approach would be to define a hysteretic energy dissipation ratio β and an overstrength factor f for the type of connection used, as was done above, such that the connections may be considered a primary source of energy dissipation. This would work well provided that the connection behaviour is consistent, repeatable, and will provide enough energy dissipation to the system. The BPC demonstrated a generally stable and predictable response, but the results presented for the SPC demonstrate that such a detail may not have a response that can be easily estimated with certainty.

This first approach is illustrated in Figure 6(a), from which the following equation for the energy dissipation ratio, β, was derived assuming rigid-rocking behavior when the load is transferred into the CRSBF at the uplifting end:
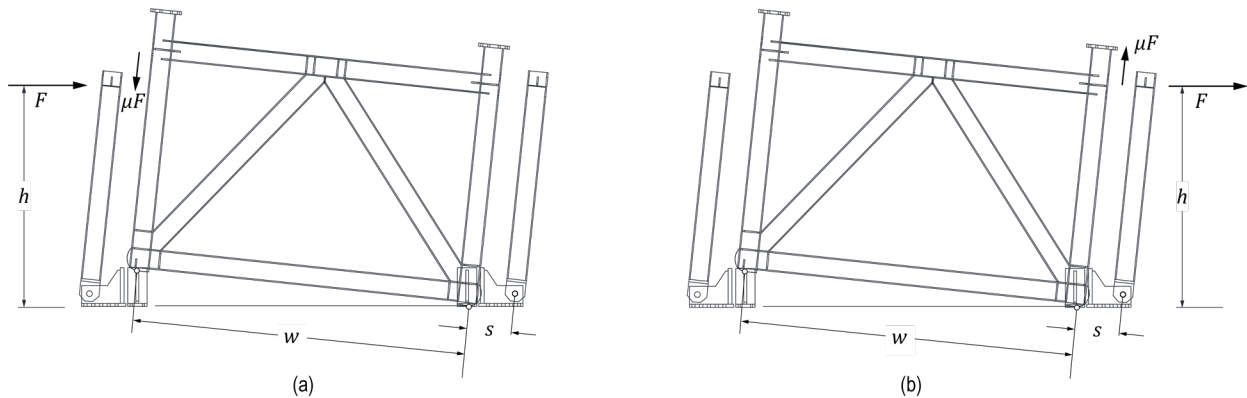
$$\beta = \frac{2\mu F(w + s/2)}{Fh} \tag{1}$$

Figure 6. Transfer of inertial force from gravity framing to CRSBF at (a) uplifting end and (b) non-uplifting end.

6

where F is the lateral load transferred from the gravity framing into the CRSBF, w is the width of the CRSBF, h is the height above the base at which the lateral load is transferred into the CRSBF, and s is the centre-to-centre spacing between the CRSBF vertical strut and the adjacent gravity column. The expression can be simplified by noting that at incipient rocking F is equal to the design base shear, V, and Fh is equal to the minimum base overturning moment, $M_{b,min}$:

$$\beta = \frac{2\mu V(w + s/2)}{M_{b,min}} \qquad (2)$$

A second approach is to minimize the influence of the connections on the hysteretic behaviour of the CRSBF such that their properties may have a negligible contribution to the overall hysteretic behaviour of CRSBFs when designing the base rocking joint. Based on Equation (1), there would be two ways to do this for a set of calculated seismic forces. First, one could try to reduce the coefficient of friction, μ, such that the connection force resisting overturning is reduced. However, this is difficult to accomplish practically with traditional construction materials, even when the components are lubricated. Second, one could reduce the moment arm to the connection from the rocking toe of the frame, which could be done by transferring the forces into the CRSBF at the side that does not uplift rather than at the uplifting side; doing so would reduce the distance over which the force resisting overturning does work to dissipate energy, and reduce its influence on the hysteretic response of the CRSBF. When the load is instead transferred at the non-uplifting end, the hysteretic energy dissipation ratio can be calculated as:

$$\beta = \frac{\mu V s}{M_{b,min}} \qquad (2)$$

This concept was used to revise the force transfer mechanism of the SPC. The pin in the connection at the North was removed and additional push-return tests were carried out on the frame with only the connection at the South end. This test was repeated in the reverse direction after the pin was moved to the North end instead. Figure 7 shows the push-only and pull-only tests plotted together for the CRSBF under 270 kN and 405 kN of vertical force. The result is a hysteresis with a flat flag shape with little energy dissipation, which more closely resembles a bilinear-elastic response than a full flag-shape. Through this mechanism, the SPC can be used to transfer the forces at the non-uplifting end of the CRSBF as described previously and thereby reduce the influence of the SPC on the overall response of the subassembly. In the tests completed for this study, the centre-to-centre spacing between the gravity and CRSBF vertical struts, s, was equal to 543 mm and the frame width, w, was equal to 4356 mm. From Equations (2) and (3), one would estimate that the connection would dissipate 94% less energy through the revised mechanism; based on the experimental results, the revised mechanism reduced the energy dissipated by approximately 88% when comparing only the push portion of the hysteresis.
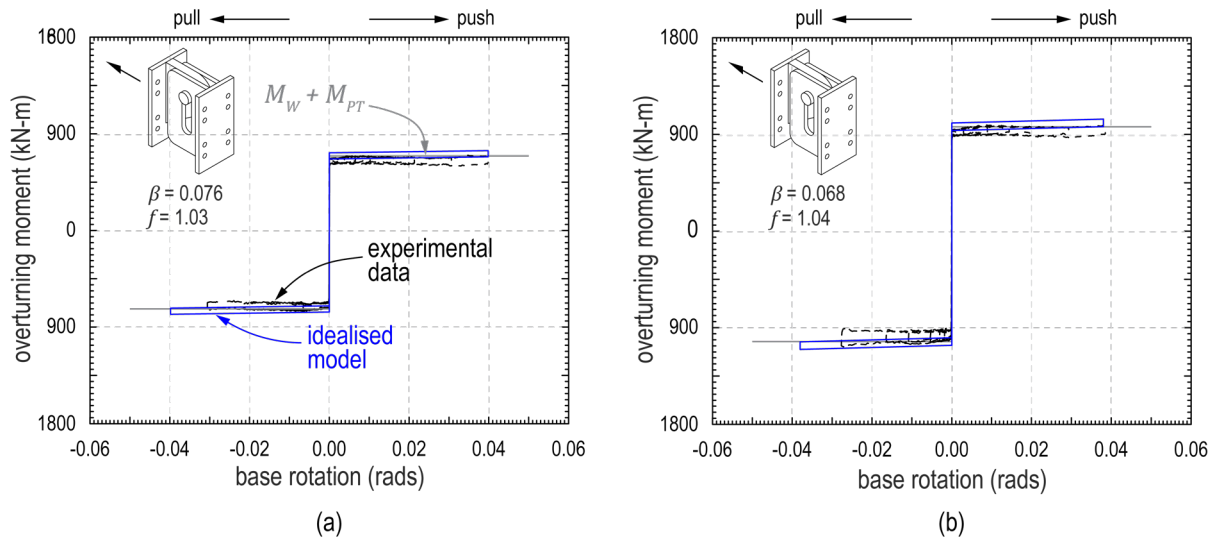

Figure 7. Cyclic static results for SPC load transfer at non-uplifting end under (a) 270 kN and (b) 405 kN of vertical load.

CONCLUSIONS

This paper presented the experimental results for two floor-to-frame connection options, both of which were intended to be low-damage solutions without requiring replacement after an earthquake. The bearing plate connection (BPC) was effective at transferring the lateral forces into the frame in bearing only; this response was generally stable and predictable, making it a good option should designers wish for the connections to contribute to the energy dissipation and overturning resistance of the

CRSBF. The energy dissipated by this connection was equal to that which would be provided by a supplemental energy dissipation device for a system design using a β value of approximately 0.36. The uplift of the opposing CRSBF vertical strut was accommodated at base rotations of up to 0.04 rad without any degradation in the strength or stiffness of the system. The maximum lateral drift was limited by both the stroke of the vertical hydraulic actuators used and the sliding distance in the connection before the bearing plate surpassed the bearing surface. However, the only limit in practice would be in the connection, and this maximum sliding distance could be increased should this be deemed necessary. Because the vertical displacements were limited by the stroke of the actuators, no results were obtained for the response of the system when the sliding distance is exceeded, so this would need to be addressed through future research.

The sliding pin connection (SPC) was effective at transferring the forces into the CRSBF either at the uplifting end or the non-uplifting end of the frame, but the response while transferring the force at the uplifting end of the CRSBF was less predictable due to the bearing and scraping of the bearing surface on the side plates. The behaviour of the connection when transferring the force at the non-uplifting end was predictable, stable, and desirable for situations where designers may want to be able to neglect the behaviour of the connections when designing the energy dissipation and post-tensioning. This revised mechanism exhibited approximately 12% of the energy dissipation and overturning resistance compared to when the force was transferred at the uplifting end, primarily because the distance over which the sliding of the pin did work relative to the bearing surface was much smaller. A symmetric response can be achieved in the pull direction by removing the bearing surface at the CRSBF side of the slotted hole, or by offsetting it such that the pin would not contact the side plates at the uplifting end.

ACKNOWLEDGMENTS

REFERENCES

[1] Steel Construction New Zealand. (2015). *Design Guide for Controlled Rocking Steel Braced Frames*. Report No. SCNZ - 110:2015, Steel Construction New Zealand, Christchurch, New Zealand.

[2] Gledhill, S. M., Sidwell, G. K., and D. K. Bell. (2008). "The damage avoidance design of tall steel frame buildings – Fairlie Terrace student accommodation project, Victoria University of Wellington." In.*2008 NZSEE Conference*, Wairakei, NZ.

[3] Tait, J. D., Sidwell, G. K., and J. F. Finnegan. (2013). "Case study – Elevate Apartments – A rocking 15 storey apartment building." In. *Steel Innovations Conference 2013*, Christchurch, NZ.

[4] Mar, D. (2010). "Design examples using mode shaping spines for frame and wall buildings." In *9th U.S. National and 10th Canadian Conference on Earthquake* Engineering, Toronto, ON.

[5] Mottier, P., Tremblay, R., and Rogers, C. (2018). "Seismic retrofit of low-rise steel buildings in Canada using rocking steel braced frames." *Earthquake Engineering and Structural Dynamics*, 47(2), 333–355.

[6] Eatherton, M. R., Ma, X., Krawinkler, H., Mar, D., Billington, S., Hajjar, J., and Deierlein, G. (2014). "Design concepts for controlled rocking of self-centering steel-braced frames." Journal of Structural Engineering, 140(11), 4014082 1–10.

[7] Wiebe, L., Christopoulos, C., Tremblay, R., and Leclerc, M. (2013). "Mechanisms to limit higher-mode effects in a controlled rocking steel frame 1: Concept, modelling, and low-amplitude shake table tests." *Earthquake Engineering and Structural Dynamics*. 42(13), 1053–1068.

[8] Eatherton, M.R., Hajjar, J.F. (2010). *Large-scale cyclic and hybrid simulation testing and development of a controlled rocking steel building system with replaceable fuses*. Report NSEL-015, Newmark Structural Engineering Laboratory, Urbana, IL.

[9] Ma, X., Krawinkler, H., and Deierlein, G. (2011). *Seismic design and behaviour of self-centering braced frames with controlled rocking and energy dissipating fuses*. Report 174, John A. Blume Earthquake Engineering Center, Stanford, CA.

[10] Roke, D., Sause, R., Ricles, J.M., and Chancellor, N.B. (2010). *Damage-free self-centering concentrically-braced frames*. ATLSS Report 10-09, Advanced Technology for Large Structural Systems Engineering Research Center, Bethlehem, PA.

[11] Latham, D.A., Reay, A.M., and Pampanin, S. (2013). "Kilmore Street Medical Centre: Application of a post-tensioned steel rocking system." In *2013 Steel Innovations Conference*, Christchurch, New Zealand.

[12] National Institute of Standards and Technology (NIST). (2010). *Evaluation of the FEMA P695-methodology for quantification of building seismic performance factors*. Report NIST GCR 10-917-8, Gaithersburg, MD.

[13] Wiebe, L. and Christopoulos, C. (2013). "Performance-based seismic design of controlled rocking steel braced frames. I: Methodological framework and design of base rocking joint." *Journal of Structural Engineering*. 141(9), 04014226 1-10.

[14] Steele, T.C., and Wiebe, L. (2016). "Dynamic and equivalent static procedures for capacity design of controlled rocking steel braced frames." *Earthquake Engineering and Structural Dynamics,* 45(14), 2349-2369.